



Role of Multiparametric-MRI in Bladder Cancer

Laura Eusebi¹ · Federica Masino^{2,3} · Rossella Gifuni^{2,3} · Davide Fierro⁴ · Michele Bertolotto⁵ · Maria Assunta Cova⁵ · Giuseppe Guglielmi^{2,3,6}

Accepted: 30 January 2023 / Published online: 27 February 2023
© The Author(s) 2023

Abstract

Purpose of Review This narrative review article aims to show the actual role of imaging, in particular MRI, and the role of VI-RADS Score, in recognition and follow-up of the tumor.

Recent Findings A team of professionals created VI-RADS with the goal of standardizing the acquisition and interpretation of multiparametric-MRI in bladder cancer.

Summary Bladder cancer is the most common cancer involving the urinary system. It is the fourth most common urological cancer in men and the second most frequent cancer affecting the urinary tract. Main risks factors are advanced age, male sex, and cigarette smoking. Bladder cancer ranges from unaggressive and usually non-invasive tumors that recur and commit patients to long-term invasive surveillance, to aggressive and invasive tumors with high disease-specific mortality. At the time of diagnosis, 70% of patients are experiencing non-muscle-invasive bladder cancer. Vesical imaging-reporting and data system score (VI-RADS) is a scoring system useful to standardize the approach to multiparametric-MRI interpretation, and reporting for bladder cancer.

Keywords Bladder cancer · Bladder imaging · Magnetic resonance imaging · Vesical imaging-reporting and data system score

Introduction

Bladder Anatomy

The bladder is a sub-peritoneal, hollow muscular organ that acts as a reservoir for urine. It is typically able to hold up to

500 ml of urine. The distended bladder has a round or oval form with a peritoneum-covered dome.

Anatomically, the bladder, contiguous with the ureters above and the urethra below, is divided into four anatomical parts: the apex or dome, body, fundus, and neck.

The apex of the bladder is directed antero-superiorly; the bladder neck is positioned inferiorly.

The internal urethral orifice is located at the bladder neck, precisely at the inferior angle of the trigone. The ureters traverse a short, oblique, intramuscular course before opening at the posterolateral angles of the trigone at the ureterovesical junction [1, 2].

The microscopic structure of the urinary bladder wall organizes into the following layers from inside out:

- Lining epithelium, the so-called urothelium, is made up of transitional cells. The urothelium is set exclusively in urinary structures (ureter, urinary bladder, and proximal urethra). In a relaxed urinary bladder, the urothelium is five to seven layers thick. When the urinary bladder fills with urine, the bladder wall stretches to accommodate the increased volume.

✉ Giuseppe Guglielmi
giuseppe.guglielmi@unifg.it

¹ Radiology Unit, “Carlo Urbani” Hospital, Via Aldo Moro 52, 60035 Jesi, AN, Italy

² Department of Clinical and Experimental Medicine, Foggia University School of Medicine, Viale L. Pinto 1, 71121 Foggia, FG, Italy

³ Radiology Unit, “Dimiccoli” Hospital, Viale Ippocrate 15, 70051 Barletta, BT, Italy

⁴ Radiology Unit, Nuovo Ospedale Dei Castelli”, Via Nettunense, Km 11/5, 00040 Ariccia, RM, Italy

⁵ Radiology Unit, “Ospedale Di Cattinara”, Trieste University, Strada di Fiume, 34149 Trieste, TS, Italy

⁶ Radiology Unit, “Casa Sollievo della Sofferenza” Hospital, Viale Cappuccini 2, 71013 San Giovanni Rotondo, FG, Italy

- Lamina propria or submucosa, a subepithelial connective tissue, contains muscle fibers with variable disposition.
- Muscularis propria, or detrusor muscle, is a smooth muscle composed of three layers (inner longitudinal, middle circular, and outer longitudinal).
- Serosa, a thin connective tissue layer, covers the bladder dome and is continuous with the peritoneal layer of the abdominal wall. It also contains blood vessels of different sizes.
- The adventitia, a layer of loose connective tissue, acts as the outer layer of the bladder in areas of the bladder where there is no serosa [3].
- superficial or papillary form, non-muscle-invasive bladder cancer (NMIBC),
- non papillary form, muscle-invasive bladder cancer (MIBC).

Bladder Cancer

Bladder Cancer is the most common cancer involving the urinary system.

More precisely, it represents the fourth cause of malignant tumors in males (after prostate, lung, and colon), while in Europe, it is among the 5–10% of all types of cancer in men (3–4 times more common than in women). The average age of onset is between 65 and 70 years [4].

The main risk factor is cigarette smoking. Even if the association between smoking and bladder cancer is present, it is not as decisive as that between smoking and lung cancer [5].

Other risk factors include exposure to occupational carcinogens (such as β -naphthylamine, benzidine, and 4-aminobiphenyl) in textile companies, in industries that produce rubber tires and paints; radiotherapy; schistosomiasis; chronic infections of the renal excretory tract (squamous cell carcinoma); and cyclophosphamide (mainly linked to urothelial carcinoma) [6].

From the histological point of view, 90% of bladder-related carcinomas are of the urothelial type, meaning they arise from transitional cells. Squamous carcinomas affect 6–8% of cases. Adenocarcinomas are rare and typically are neoplasms that develop from urachus residues.

In about 25% of urothelial carcinomas, there is a mixed histology, which includes neuroendocrine, small cell, micropapillary, sarcomatous, and plasmacytoid components. The prognosis of these variants is worse than that of pure urothelial carcinoma [7].

From an anatomopathological point of view we distinguish

- grade 1, well differentiated,
- grade 2, moderately differentiated,
- grade 3, poorly differentiated.

Bladder cancer is morphologically classified into

The *NMIBC* form is more frequent (70–80%) [8]. In two thirds of cases, it occurs as a low-grade papillary form that originates from the hyperplastic epithelium and is limited to the mucosa and lamina propria. It has a good prognosis, despite its multicentricity and its possibility of recurrence after surgical removal (70% after 3 years). These are typical traits of this form, which can progress to a muscle-invasive form if untreated [9]. The superficial form is present in the remaining one-third of cases and is characterized by the presence of a flat, high-grade, malignant carcinoma in situ, which can rapidly invade the muscle plane and metastasize.

The *MIBC* form (20–30%) is typically characterized by a poor prognosis, due to the rapid infiltration of the different layers of the bladder wall and outside the bladder [7]. These are frequent multifocal forms, and about 2–5% of patients with bladder cancer have a similar neoplasm in the remaining tracts of the excretory system in a synchronous or metachronous manner. The invasive forms spread by the lymph node, with initial involvement of the locoregional lymph nodes and, subsequently, of the common iliac, paracaval and lumbo-aortic chain. Lung, bone, liver, and adrenal glands are most frequently affected by blood-borne metastasis [10•]. Furthermore, these tumors high-frequently relapse, a condition that requires stringent post-therapeutic monitoring process known as “urothelial surveillance.”

The onset symptom is the so-called “Painless Hematuria,” both micro and macro hematuria, asymptomatic. This is typically terminal hematuria in 85% of patients, which can be clinically distinguished from prostatic hematuria (hematuria in the initial phase of urination, with subsequent clearing of the urine) [11]. Late symptoms include pollakiuria, obstruction of regular urination, pelvic pain, and urinary tract infection. Concerning bladder tumor treatment, the *NMIBC* form is a cancer usually managed with transurethral resection bladder tumor (TURBT) and in some cases with intravesical therapy, such as the administration of *Bacillus of Calmette–Guérin* (BCG). Bladder function is preserved [5, 12••]. Radical cystectomy is typically used to treat *MIBC* forms. Neoadjuvant therapy, which uses new chemotherapeutic and in particular immunotherapeutic drugs, opens up a new therapeutic frontier [4, 13, 14].

Bladder Cancer Staging

The staging system most often used for bladder cancer is the American Joint Committee on Cancer (AJCC) tumor–node–metastasis (TNM) system, summarized in Table 1. The last edition was the 8th, updated in 2017 [12••].

Table 1 The 8th edition of the TNM system, the most used for bladder cancer's staging

T	Primary tumor
TX	Primary tumor cannot be assessed
T0	No evidence of primary tumor
Tis	Carcinoma in situ
T1	Tumor invades subepithelial connective tissue layer
T2	Tumor invades: T2A: superficial muscle T2B: deep muscle
T3	Tumor invades perivesical tissue T3A: microscopically T3B: macroscopically (extravesical mass)
T4	Tumor invades the following: T4A: prostatic stroma, seminal vesicles, uterus or vagina T4B: pelvic wall or abdominal wall
N	Regional lymph nodes
NX	Regional lymph nodes cannot be assessed
N0	No regional lymph nodes metastasis
N1	Metastasis in a single lymph node in the true pelvis, involving perivesical lymph nodes
N2	Metastasis in multiple regional lymph nodes in true pelvis
N3	Metastasis in common iliac lymph node(s)
M	Distant metastasis
M0	No distant metastasis
M1	M1A: Non-regional lymph nodes only M1B: Non-lymph-node distant metastasis

The *NMIBC* form is sub-classified into

- TA, non-invasive papillary carcinoma.
- T1S, non-invasive carcinoma in situ.
- T1, invasion of the lamina propria.

The *MIBC* is sub-classified into

- T2A, with invasion of the superficial half of the detrusor.
- T2B, with invasion of the deep half of the detrusor.
- T3A, with microscopic invasion of the perivesical fat.
- T3B, with macroscopic invasion of the perivesical fat.
- T4, with extravesical diffusion, so with infiltration of the pelvic organs or the abdominal wall (Fig. 1).

T2B has a worse prognosis, due to a higher risk of lymph node metastases (30% T2B versus 14% T2A) and a reduced free survival after cystectomy. Radiological imaging cannot distinguish between the two entities; however, the therapeutic strategy is the same for both T2A and T2B.

In addition to the type of bladder cancer, risk stratification is influenced by the number and size of the lesions, the occurrence of the first relapse, the presence of concurrent carcinoma in situ, and the level of neoplasm [13].

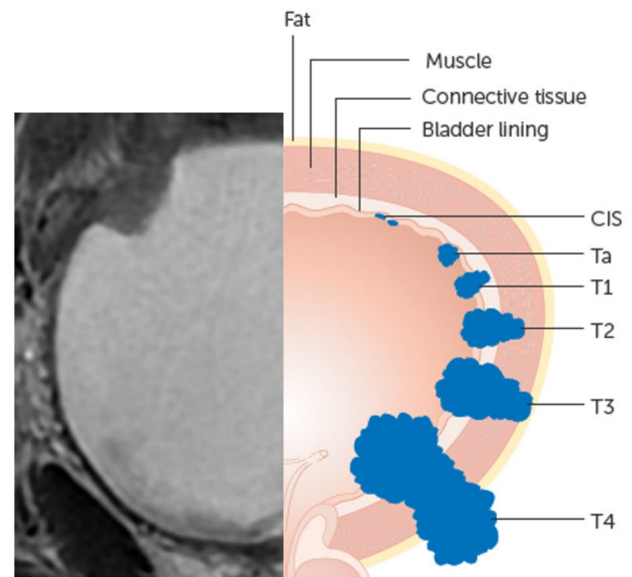


Fig. 1 On the right graphical representation of the different stages of bladder cancer, compared with a T2 MRI of the bladder on the left

Imaging

The role of imaging in the diagnosis and staging of bladder cancer is critical [14].

The initial diagnostic approach to the patient at risk includes clinical evaluation, urinalysis, ultrasonography, and cystoscopy. Through TUR (transurethral endoscopic resection), anatomopathological findings are obtained. These findings range from grade 1, well-differentiated forms, to grade 3, poorly differentiated forms [15]. TUR is also used to assess the degree of tumor depth in the bladder wall and the possible infiltration of the detrusor muscle, thus allowing a differential diagnosis between a T1 and a T2, with a significant change in the therapeutic approach. Recent studies have shown that 40% of TUR results are false negatives because of tumor micro residues, which can lead to local recurrence and distant metastases. Modern imaging, which aims to both detect the neoplasm and to distinguish the *NMIBC* forms from the *MIBC* ones, is specifically inserted in this perspective [16].

Multiparametric Ultrasound

On ultrasound, the bladder wall is made up of three different layers: the hyperechoic outer serosa, the detrusor muscle with its medium homogeneous echogenicity, and the hyperechoic inner mucosa. The bladder content is anechoic [17].

Ultrasound has a high detection rate (90–95% of cases), in the presence of vegetative with dimensions greater than 5 mm, located in the lateral and posterior walls of the bladder [18].

However, on US, infiltrative tumors may be not diagnosed or it may be difficult to differentiate them from non-neoplastic lesions.

The main limit of ultrasound is its inability to detect small, flat, and plaque lesions, especially when they are located at the fundus, or when they are hidden by the presence of large prostatic adenomas. Even benign conditions, such as columnar hyperplasia or prostatic hypertrophy, can cause false positives and false negatives. Therefore, the lesion's location may represent an important obstacle to the detection of the lesion itself, leading to underdiagnosis [19].

The vascularization of the lesion on ultrasound is studied through echo-color-Doppler (ECD) and contrast-enhanced ultrasound (CEUS), useful to distinguish it from a possible clot.

With a higher frequency transrectal ultrasound (TRUS) in men, or with a vaginal probe in women, the bladder fundus as well as the distal and intramural part of the ureter can be seen during an endosonographically examination, with patient in lithotomy position. Transurethral ultrasound is probably the best method for determining the extent of a tumor's invasion into the bladder wall and for differentiating superficial and deeply infiltrating tumors. Limiting the latter examination, compared to the classic US, is that it is an invasive technique [20].

CT-Urography

CT-urography (CTU) is the most frequently used method in the diagnosis and staging of bladder cancer, due to its high availability and excellent cost–benefit ratio.

CTU may be performed with three different approaches: the single-bolus, the split-bolus, and the triple bolus.

The first, the single-bolus, is the most used. This technique requires an unique full-strength bolus of contrast medium and the acquisition of arterial, venous, and excretory phase images.

In the split-bolus method, the total contrast material is divided into two administrations, while images are acquired in a combined excretory and nephrographic phase. In order to better highlight the renal/urothelial parenchyma, the exam is conducted in two phases: a non-contrast phase is followed by a single urothelial and excretory phase exam that is conducted after providing a partial bolus, waiting for excretion, and then administering the remaining dose.

The triple bolus technique allows a combined acquisition of corticomedullary-nephrographic-excretory phase.

It is crucial to know that the split-bolus and triple-bolus procedures were created primarily to lower radiation exposure by merging the several acquisition steps [21–23].

The essential limit is the inability to distinguish between non-muscle-invasive forms from invasive muscle forms

(accuracy of about 91% in detection, but only 35–55% in local staging). In fact, the CTU does not permit determining the level of muscle wall infiltration and consequently to differentiate the T1 stage from T2, or the T2A stage from T2B. On the contrary, CTU displays an accuracy between 83 and 93% in the more advanced forms, with stage T3B and T4 and infiltration of perivesical fat [24••].

Concerning lymph nodes evaluation (N staging), CTU enables their morphology and size assessment. Regarding size, suspect occurs when pelvic and abdominal-retroperitoneal lymph nodes have a short axis, respectively, greater than 8 mm and 10 mm. About the morphological criterion, the presence of confluent lymph nodes or those with a necrotic center is considered a clear sign of lymph node metastasis.

The limit of the CT study of the lymph nodes is the potential over-staging, detected in about 30% of cases with reactive lymphadenopathies with a short axis greater than 10 mm. Sub-staging is possible in case of lymph nodes with dimensions within the limits, but nevertheless the site of micro-metastases [25].

The evaluation of the urothelium of the upper excretory tracts plays a crucial role in the case of bladder carcinoma hematuria, in addition to its role to detect the extent of the disease's locoregional spread. In fact, in a percentage that varies between 2 and 5% of cases, patients with bladder cancer have a synchronous or metachronous tumor of the upper excretory tract, as well as 50% of patients with neoplasms originating from the urothelium of the upper tract, excretory presents bladder neoplasms.

Multiparametric-MRI

According to the major European and American urological associations, TURBT is the cornerstone in the diagnosis and staging of bladder cancer. However, this is a procedure that has its own diagnostic inaccuracy, considering that the persistence of the tumor is documented after resection of a T1 neoplasm in 33–50% of cases, and T3 in 40% [8, 12••, 26].

Furthermore, about one-third of the neoplasms clinically confined to the organ show an extra bladder extension to the pathological anatomy after radical cystectomy.

For this reason, MRI is acquiring an increasingly important role in the evaluation of bladder cancer as well, thanks to the development and implementation of modern equipment which, with the insertion of functional sequences, have overcome the limit of CT in differentiating between non-muscle-invasive forms from invasive muscle forms [4, 5, 27].

Due to its high multiparametric capacity, MRI is performed to study the bladder wall, and to distinguish an invasive muscle tumor from a non-muscle-invasive tumor [28, 29].

Additionally, MRI enables us to evaluate the response to neoadjuvant treatment, in order to identify complete responders and to have a correct therapeutic approach. It is an important consideration due to the increasing important role of immunotherapy today [30–32].

Some patients may not be eligible for MRIs due to possible safety issues with implanted metallic devices or foreign bodies. Low spatial resolution and signal-to-noise ratio of diffusion-weighted imaging limit its applicability for the assessment of small tumors or thin bladder wall with over-distension and make it susceptible to numerous artifacts. Moreover, transurethral resection biopsy is required for tumor grading and cannot be replaced by MRI [33, 34].

Patient Preparation

In order to optimize the examination, a proper preparation of the patient is essential. Before performing the MRI exam, it is necessary that the bladder is moderately distended by instructing patients to urinate approximately 2 h before imaging, then start drinking 500–1000 ml of water half an hour before the exam depending on the ability of the patient to hold urine. Targeted scans using the localizer can be useful before the exam to assess when the bladder is optimally full (about 300 ml).

Without adequate distension, the bladder wall may appear thickened, leading to a misdiagnosis of bladder cancer. Excessive distension can cause movement artifact due to patient discomfort or difficulty for the patient to hold urine during the course of the examination, it should in fact be considered that during the examination the volume of the bladder can increase by about 10%. In case of a history of urinary retention, the patient should follow a personalized hydration plan, while in case of insufficient repletion, the patient should drink again and postpone the examination for 30–60 min. A drug that helps relax the intestine and minimizes intestinal peristalsis can be useful in maximizing imaging yield by implementing the diagnostic capacity.

Multiparametric-MRI Technique

In our institution, MRI of the bladder was performed supine with a 1.5 T MRI scanner (Optima 450, GE Healthcare), using a sixteen-inch pelvic coil channels and phased arrays. The first sequence to be acquired is a T1W Fast Spin Echo with Cartesian filling of the K space and a wide Field of View (FoV) which are used to evaluate the adequate filling of the bladder, the pelvic excavation, and the possible involvement of the main lymph node stations (FAST SPIN ECHO; T_R/T_E 400–500/10–20, slice thickness 5 mm and intersection gap 0.5 mm) acquired in the axial plane.

Subsequently, the T2W sequences with high resolution, narrow FoV, with radial filling of the K space are

acquired which guarantee an excellent contrast resolution and a minimization of motion artifacts (PROPELLER; T_R/T_E 5000–6000/90–120, slice thickness 3.5 mm and intersection gap 0.5 mm) on the three planes of the space (axial, sagittal or coronal) and without suppression of the adipose tissue signal.

The DWI sequence acquires in the axial plane with free breathing, inviting the patient to perform superficial breaths, with single-shot eco-planar spin sequence excited with water and suppressed of the adipose tissue signal (T_R/T_E 4000/78, slice thickness 3.5 mm, intersection gap of 0.5 mm and b values of 0–500–800–1000).

Then, a quantitative evaluation of diffusion is performed against the values of the apparent diffusion coefficient (ADC, mm^2/s) which were automatically calculated by manually positioning the region of interest (ROI) within the most hypointense areas of the lesions.

Finally, the DCE-MRI was performed with the T1W three-dimensional gradient echo sequence (3D) with suppression of the adipose tissue signal using the Dixon Three Point method (LAVA FLEX; T_R/T_E 4/1.7, partition of the volume 1.4 mm, duration of the single phase less than 10 s, 25/30 phase after administration of the contrast medium).

At the end of the acquisition, perfusion maps with Wash in/Wash out and possible affixing of ROI on suspicious areas must be performed using a dedicated workstation to evaluate the vascularity and kinetics of the contrast medium.

All images should include the entire urinary bladder, proximal urethra, and prostate if the patient is a male. In females, the adjacent pelvic viscera (uterus, ovaries and vagina) should also be included.

VI-RADS Score and Performance

Due to its spatial resolution, MRI cannot fully assess the stratification of the bladder wall. Particularly, the mucosa is identifiable as a hyperintense line only in the early phase of the DCE-MRI study. On the other hand, the detrusor muscle appears as a low-signal intensity line on T2WI, with intermediate signal intensity in DWI and ADC map sequences, and late and progressive contrast enhancement in DCE-MRI [29]. The inner layer, composed of urothelium and lamina propria, is not seen using T2 and DWI, but it shows early contrast increase and appears as a hyperintense line in the arterial phase.

With a view to standardization in the acquisition and interpretation of MRI in bladder cancer, a group of experts in 2018 developed VI-RADS [17]. VI-RADS applies to patients who have never been treated (uVI-RADS) and to patients who have only had a diagnostic TURBT, before a re-TURBT (tVI-RADS) [11]. The score, with a range from

one to five, stratifies the risk related to the possible infiltration of the muscle wall.

Scores 1 and 2 are assigned to tumors with low probability of infiltrating the detrusor muscle (Fig. 2).

Score 3 expresses a dubious category, similar to the PI-RADS score in prostate cancer.

A score of 4 or 5 is assigned to tumors with a high probability of infiltrating the detrusor muscle [35] (Figs. 3, 4, 5).

According to the largest meta-analysis, considering VI-RADS 3 as infiltration cut-off, the sensitivity is higher (92%) and the specificity (85%) is lower [21]. On the other hand, considering VI-RADS 4 as infiltration cut-off, the sensitivity is lowered (82%) and the specificity rises (95%) [8, 19].

In the VI-RADS score, as well as for PI-RADS, it is necessary to consider the different information coming from the T2 sequences, from the DCE, and DWI and ADC. Therefore, each acquisition sequence generates a result for a bladder lesion that will be ranked from one to five. T2WI acquisition allows for the analysis of the structural category (SC), while DWI and ADC map are the support of the DW category, and DCE is the support of the CE category [36].

The initial evaluation is performed using T2WI to evaluate the integrity of the detrusor muscle and proceed with the SC ranging. In T2WI, the lesions present an

intermediate SI, in contrast to the low signal of the muscle layer and the high signal of the urine. An uninterrupted low signal will be the distinctive of highly predictive categories 1 and 2 of NMIBC. Often around the vegetation, there is a sort of thickening of the wall below the vegetation, and adjacent to it. In these cases, a thickened and hyperintense line is seen in T2, demonstrating the presence of edema, which represents an inflammatory reaction due to the presence of a neoformation.

VI-RADS 1 is associated to the presence of the tumor, but with less than 1 cm in size. In this case, it will rarely be an invasive muscle form, especially if it has a vegetable form, rather than a sessile.

VI-RADS 2 is reserved for stalk with more than 1 cm in size, but without invasion of the muscle layer.

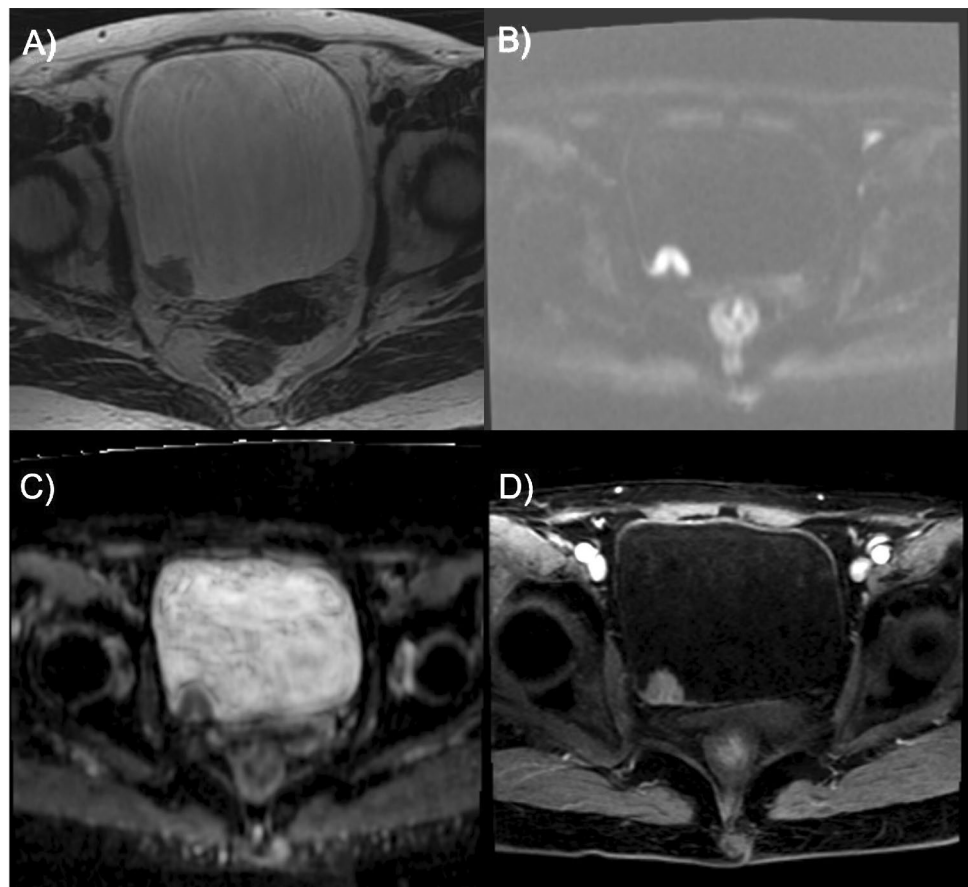
VI-RADS 3 is associated to an equivocal neoformation.

VI-RADS 4 is assigned when there is a decisive invasion of the detrusor muscle, with interruption of the low SI of the muscular layer.

VI-RADS is 5 when beyond the characteristics of 4, there is also the extension at the level of the adipose tissue.

The same approach used for the determination of the lesion through T2WI is done for DWI/ADC and DCE images.

Fig. 2 Case of a VI-RADS overall score of 2, a pT1 urothelial carcinoma confirmed on histopathology after TURBT. **A** T2WI (axial plane) showed an exophytic lesion on the right posterior bladder wall, more than 1 cm in size, with preserved low SI muscle (VI-RADS 2). **B** DWI and **C** ADC map, respectively, demonstrated a limited diffusion exophytic lesion, with low-signal pedicle (SI) on DWI and muscular own with continuous low SI on DWI (VI-RADS 2). **D** DCE imaging showed early improvement of the lesion and inner layer, without early improvement of the proper musculature (VI-RADS 2)



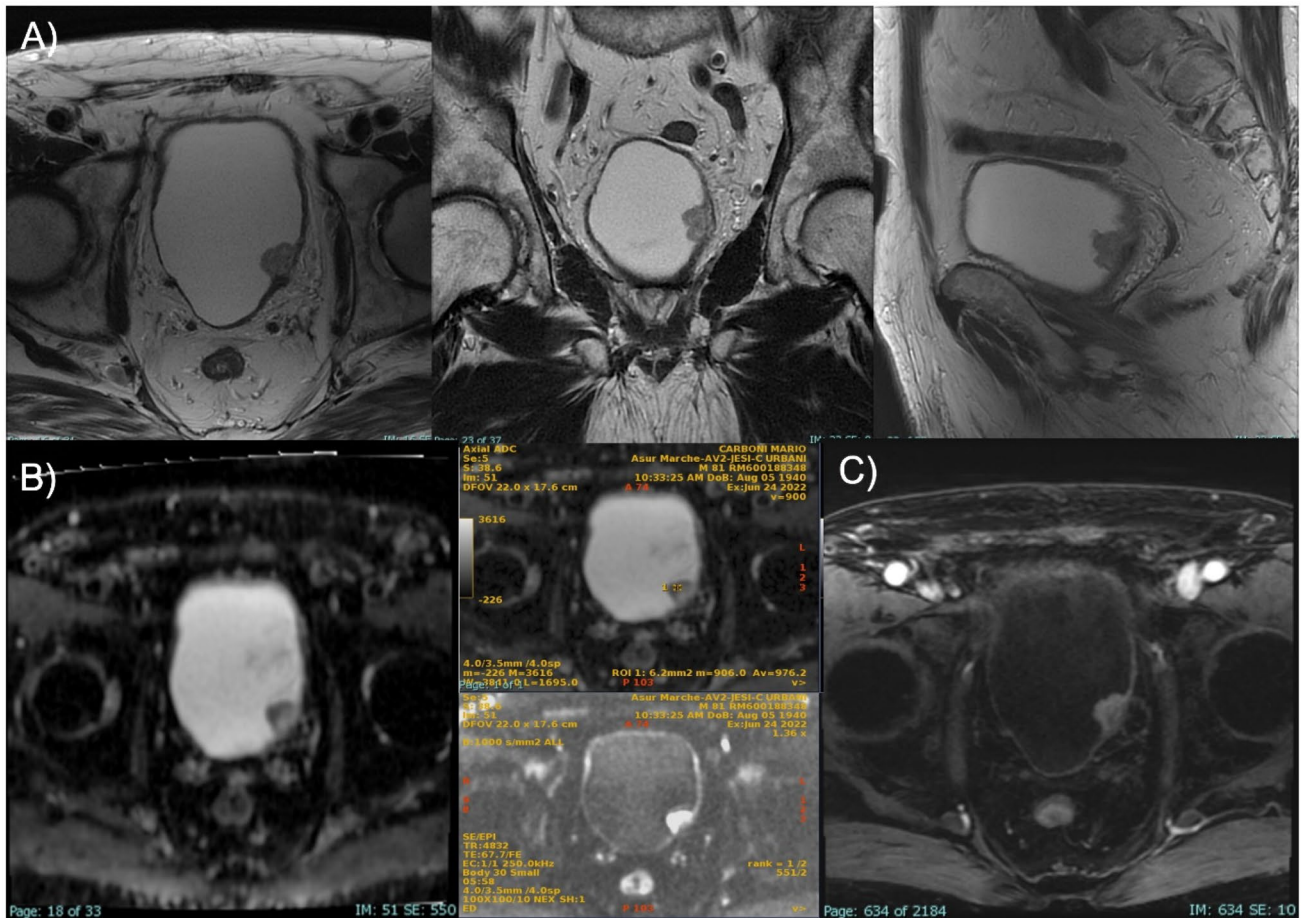


Fig. 3 Case of a VI-RADS overall score of 4. **A** T2WI (axial, coronal and sagittal plane) imaging showed a sessile mass of more than 1 cm in size at the left bladder wall, with intermediate SI extending through the proper muscle (VI-RADS 4). **B** DWI and ADC maps showed a lesion with significant limited diffusion, extend-

ing through the own muscle. The low ADC value of approximately $0.9 \times 10^{-3} \text{ mm}^2/\text{s}$ which denoted malignant nature (VI-RADS 4). **C** DCE imaging showed early and heterogeneous improvement of the lesion, extending through the own muscle (VI-RADS 4)

On DWI/ADC, muscularis propria should present an intermediate SI, while the stalk and inner layer have low SI on DWI. For high scores, the tumor appears hyperintense on DWI and hypointense on the ADC map with extension to the muscularis propria.

On DCE, muscularis propria should maintain no enhancement in the early phase; it is recognizable as a low SI line under the tumor. Cancer and inner layers early enhancement are associated with a higher score (Fig. 6).

Following this, DWI/ADC and DCE categories help to further stratify the lesion, and the overall score of VI-RADS can originate from different combinations of T2, DWI, and DCE categories. In case of a discrepancy of results between SC (T2 images) and functional sequences (DWI and DCE), these two sequences will prevail, both for downgrade and upgrade lesions [27] (Fig. 7).

The purposes of the VI-RADS Score are as follows: standardization of the acquisition protocol, improvement of image quality, greater ease in the description of findings, and reduction of interobserver variability [37]. The main advantage of VI-RADS, similarly to PI-RADS, is that it allows to standardize the approach in both acquisition and reporting, with a good intrareader agreement (K range 0.7–0.93). Furthermore, it is widely accepted by the radiology community [27].

Multiparametric-MRI After Neoadjuvant Therapy

An extremely recent topic concerns the use of MRI in post therapy control. Today, in fact, the real revolution in the treatment of bladder cancer is given by immunotherapy,

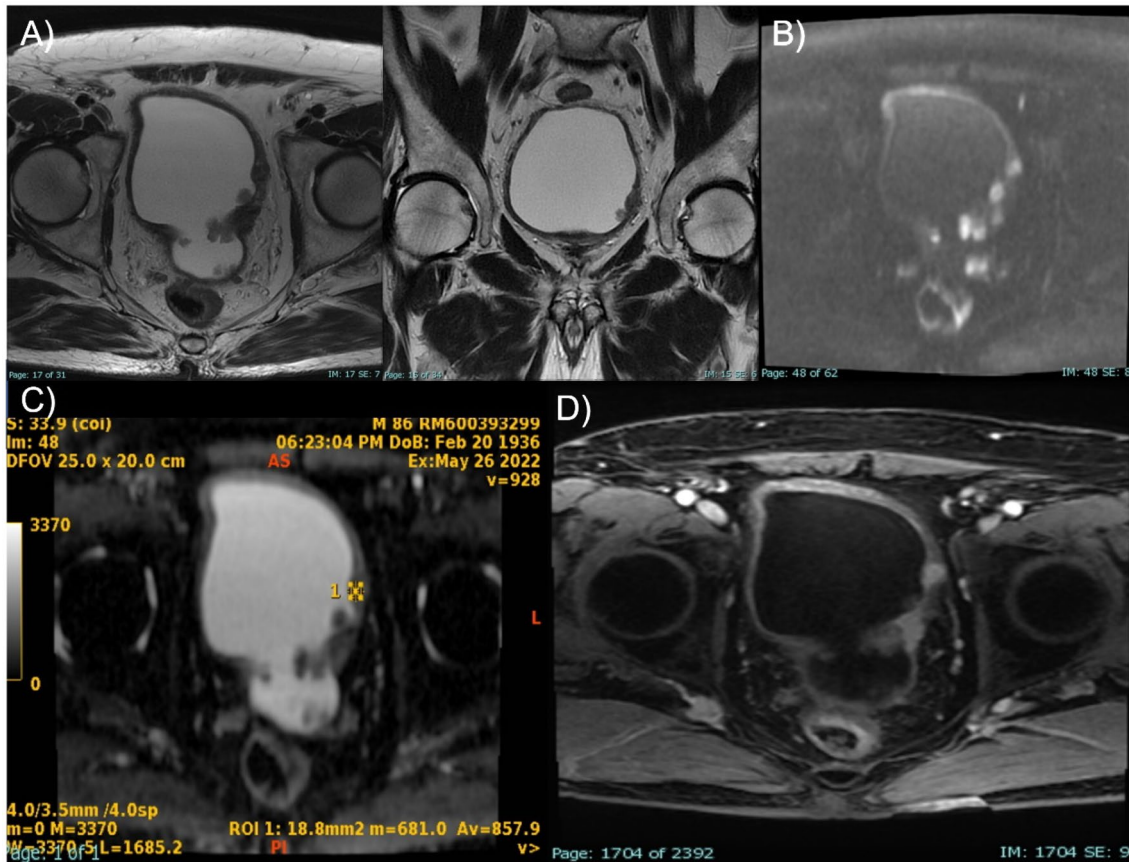


Fig. 4 Case of multifocal bladder tumors, with a VI-RADS overall score of 4. **A** The T2WI (axial and coronal plane) showed the most anterior tumor, which is an endophytic (intramural growth) tumor of the left lateral wall, with intermediate SI and with a clear extension in the proper low SI musculature (VI-RADS 4). **B** DWI showed

the corresponding high SI and intramural growth (VI-RADS 4). **C** The low ADC value of about $0.8 \times 10^{-3} \text{ mm}^2/\text{s}$ indicated malignant nature (VI-RADS 4). **D** The DCE showed an early and heterogeneous enhancement of the lesion, which extends through the own muscle DCEI (VI-RADS category 4)

which has an excellent response in patients with muscle-invasive cancer [27].

In MIBC, to determine whether a lesion still exists after neoadjuvant therapy in MIBC, it is necessary to examine the T2, DWI, and DCE sequences on MRI. Then it is evaluated if there is a response to the therapy, which can be partial, complete, or absent [26].

The future goal will be to carry out surveillance in patients with partial or complete response, combining MRI and cystoscopy, without the need for bladder resection [27].

The use of the VI-RADS score is also proposed in the evaluation of the bladder cancer response to systemic therapy [26].

Conclusion

MRI makes it possible to evaluate the invasion of the muscular plane of the bladder. Taking advantage of this ability, the VI-RADS score was designed, an algorithm with the advantage of being performing, reproducible, non-invasive and simple. All features that would make it easily applicable, only performing an MRI and evaluating T2WI, DWI, ADC, and DCE sequences. In addition to the initial stratification of bladder cancer risk by discriminating an NMIBC form from a MIBC form, the responses to post neoadjuvant therapies and bladder sparing approaches are other potential clinical applications of the score.

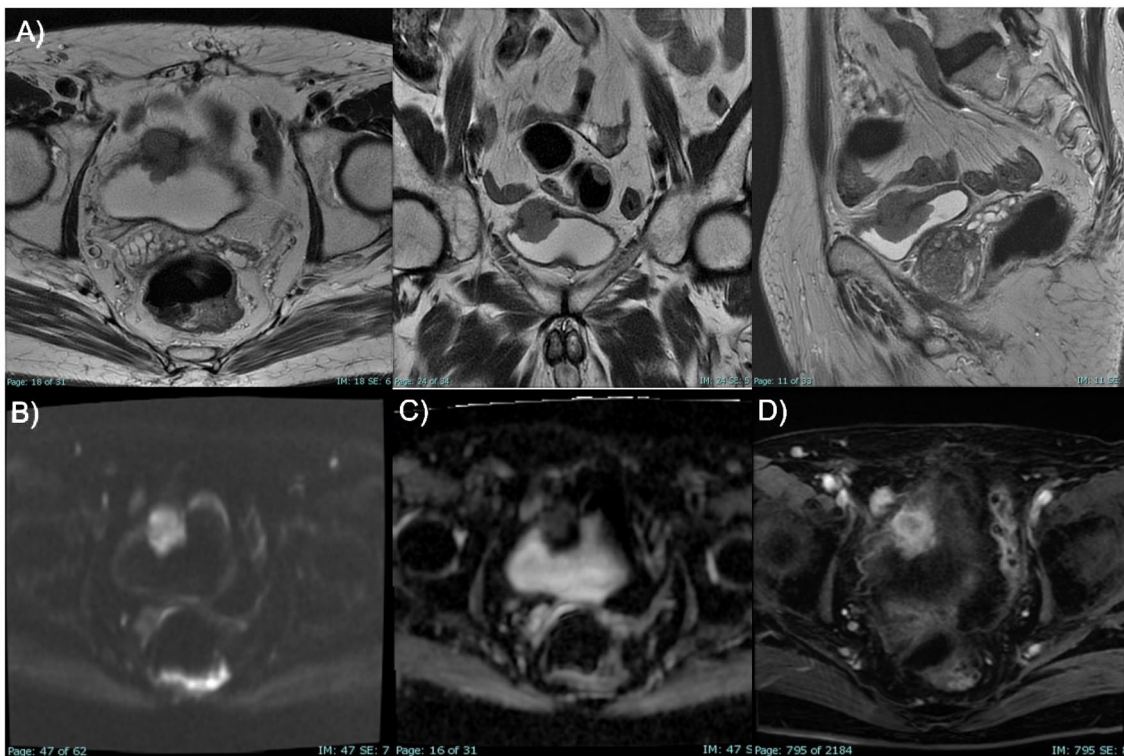


Fig. 5 Case of a VI-RADS overall score of 5. **A** T2WI (axial, coronal and sagittal plane) showed a sessile mass larger than 1 cm on the right lateral wall of the bladder dome, with an intermediate SI, extending through the proper muscle and invading the perivesical adipose tissue (VI-RADS 5). **B** DWI and **C** ADC map showed a

significantly limited diffusion lesion extending through the muscularis propria invading the perivesical adipose tissue (VI-RADS 5). **D** DCE showed an early and heterogeneous improvement of the lesion extending through the invading proper muscle the perivesical adipose tissue (VI-RADS 5)

Fig. 6 How to interpret MRI-sequences to obtain the VI-RADS overall score

	T2WI	DCE	DWI	ADC	
Uninterrupted low SI line representing muscularis integrity < 1,0 cm size.					VI-RADS 1
Uninterrupted low SI line representing muscularis integrity > 1,0 cm size and thickened inner layer					VI-RADS 2
Disappearance of category 2 findings, but no clear disruption of low SI muscularis layer					VI-RADS 3
Interruption of low SI line suggesting extension into muscularis layer					VI-RADS 4
Extension of intermediate SI tumor to extra-vesical fat					VI-RADS 5

Stalk

Cancer

Inner layer (IL)

Muscularis

Cancer & IL

Stalk

Muscularis

Cancer Stalk & IL

Muscularis

Cancer & IL

Stalk

Muscularis

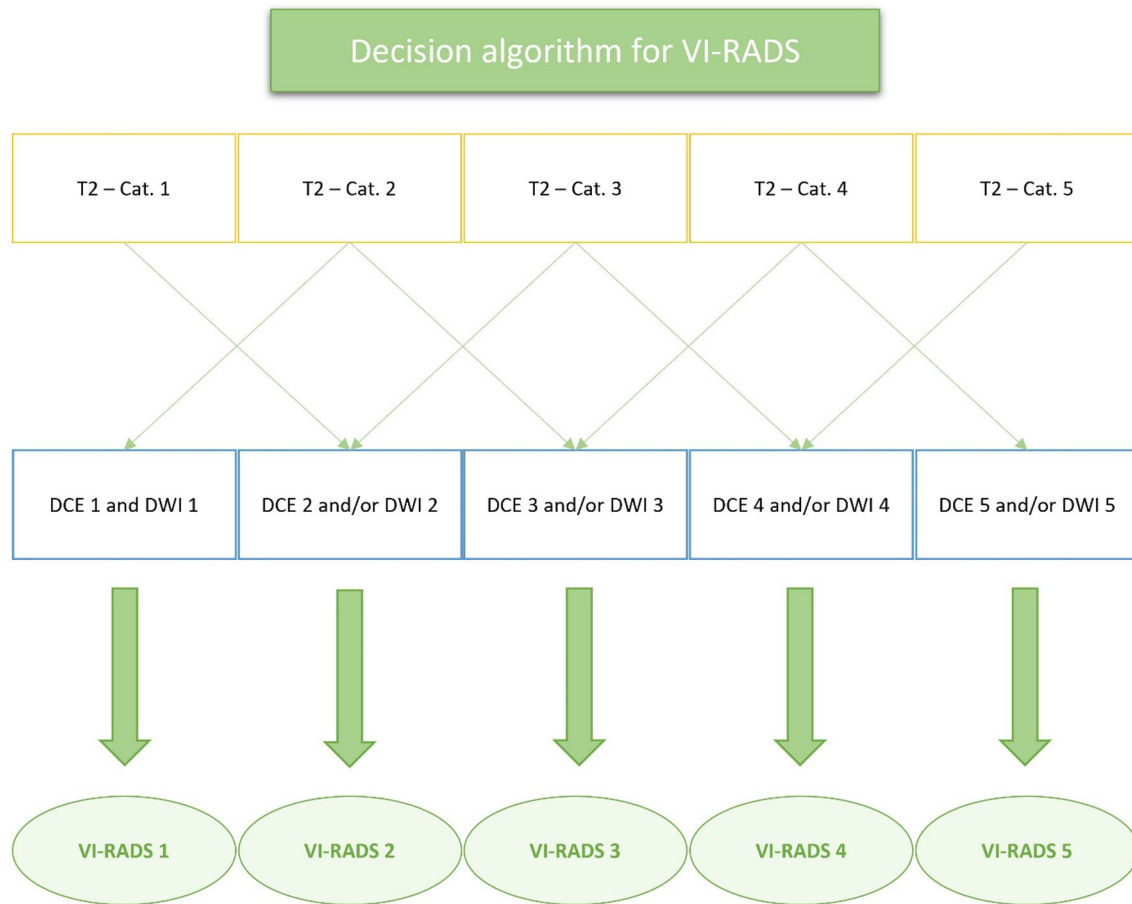


Fig. 7 The decision algorithm for VI-RADS, obtained by the combination of T2 images and DCE and DWI

Acknowledgements We thank Dr. Emilio Quaia for reviewing the manuscript

Author Contributions All authors contributed to the article conception and design. All authors read and approved the final manuscript.

Funding Open access funding provided by Università di Foggia within the CRUI-CARE Agreement.

Data availability The authors declare that the data supporting the findings of this study are available within the article.

Declarations

Conflict of interest The authors have no financial or competing interests to disclose.

Ethical Approval This article does not contain any studies with human or animal subjects performed by any of the Authors.

Open Access This article is licensed under a Creative Commons Attribution 4.0 International License, which permits use, sharing, adaptation, distribution and reproduction in any medium or format, as long as you give appropriate credit to the original author(s) and the source, provide a link to the Creative Commons licence, and indicate if changes were made. The images or other third party material in this article are

included in the article's Creative Commons licence, unless indicated otherwise in a credit line to the material. If material is not included in the article's Creative Commons licence and your intended use is not permitted by statutory regulation or exceeds the permitted use, you will need to obtain permission directly from the copyright holder. To view a copy of this licence, visit <http://creativecommons.org/licenses/by/4.0/>.

References

Papers of particular interest, published recently, have been highlighted as:

- Of importance
- Of major importance

1. Shinagare AB, Sadow CA, Sahni VA, Silverman SG. Urinary bladder: normal appearance and mimics of malignancy at CT urography. *Cancer Imaging*. 2011;11(1):100–8. <https://doi.org/10.1102/1470-7330.2011.0017>. (Published 28 June 2011).
2. Sam P, Nassereddin A, LaGrange CA. Anatomy, abdomen and pelvis, bladder detrusor muscle. In: StatPearls. Treasure Island: StatPearls Publishing; 2021.
3. Bolla SR, Odeluga N, Jetti R. Histology, bladder. In: StatPearls. Treasure Island: StatPearls Publishing; 2022.

4. Antoni S, Ferlay J, Soerjomataram I, Znaor A, Jemal A, Bray F. Bladder cancer incidence and mortality: a global overview and recent trends. *Eur Urol*. 2017;71(1):96–108. <https://doi.org/10.1016/j.eururo.2016.06.010>.
5. Rozanec JJ, Secin FP. Epidemiología, etiología, prevención del cáncer vesical [Epidemiology, etiology and prevention of bladder cancer]. *Arch Esp Urol*. 2020;73(10):872–8.
6. Farling KB. Bladder cancer: risk factors, diagnosis, and management. *Nurse Pract*. 2017;42(3):26–33. <https://doi.org/10.1097/01.NPR.0000512251.61454.5c>.
7. Kamoun A, de Reyniès A, Allory Y, et al. A consensus molecular classification of muscle-invasive bladder cancer. *Eur Urol*. 2020;77(4):420–33. <https://doi.org/10.1016/j.eururo.2019.09.006>.
8. Babjuk M, Burger M, Capoun O, et al. European Association of Urology guidelines on non-muscle-invasive bladder cancer (Ta, T1, and carcinoma in situ). *Eur Urol*. 2022;81(1):75–94. <https://doi.org/10.1016/j.eururo.2021.08.010>.
9. Babjuk M, Böhle A, Burger M, et al. EAU guidelines on non-muscle-invasive urothelial carcinoma of the bladder: update 2016. *Eur Urol*. 2017;71(3):447–61. <https://doi.org/10.1016/j.eururo.2016.05.041>.
10. ●Wang Z, Shang Y, Luan T, et al. Evaluation of the value of the VI-RADS scoring system in assessing muscle infiltration by bladder cancer. *Cancer Imaging*. 2020;20(1):26. Published 6 April 2020. <https://doi.org/10.1186/s40644-020-00304-3>. *Important reference which reinforces the good diagnostic value in predicting the degree of tumor invasion of VI-RADS and therefore in bladder cancer management.*
11. Matulewicz RS, Rademaker A, Meeks JJ. A simplified nomogram to assess risk of bladder cancer in patients with a new diagnosis of microscopic hematuria. *Urol Oncol*. 2020;38(4):240–6. <https://doi.org/10.1016/j.urolonc.2019.12.010>.
12. ●●Wong VK, Ganeshan D, Jensen CT, Devine CE. Imaging and management of bladder cancer. *Cancers (Basel)*. 2021;13(6):1396. Published 19 March 2021. <https://doi.org/10.3390/cancers13061396>. *Reference useful to have a panoramic view of imaging role in the diagnosis and follow-up of bladder cancer, including multiparametri-MRI.*
13. ●Jazayeri SB, Dehghanbanadaki H, Hosseini M, et al. Diagnostic accuracy of vesical imaging-reporting and data system (VI-RADS) in suspected muscle invasive bladder cancer: a systematic review and diagnostic meta-analysis. *Urol Oncol*. 2022;40(2):45–55. <https://doi.org/10.1016/j.urolonc.2021.11.008>. *ThehighdiagnosticaccuracyofVI-RADStopredictMIBCiswell explained in this article as well.*
14. Bicchetti M, Simone G, Giannarini G, et al. A novel pathway to detect muscle-invasive bladder cancer based on integrated clinical features and VI-RADS score on MRI: results of a prospective multicenter study. *Radiol Med*. 2022;127(8):881–90. <https://doi.org/10.1007/s11547-022-01513-5>.
15. Paner GP, Stadler WM, Hansel DE, Montironi R, Lin DW, Amin MB. Updates in the eighth edition of the tumor–node–metastasis staging classification for urologic cancers. *Eur Urol*. 2018;73(4):560–9. <https://doi.org/10.1016/j.eururo.2017.12.018>.
16. Gadzinski AJ, Psutka SP. Risk stratification metrics for bladder cancer: Comprehensive Geriatric Assessments. *Urol Oncol*. 2020;38(9):725–33. <https://doi.org/10.1016/j.urolonc.2020.01.003>.
17. Kim SH, Cho JY, Lee HJ, Sung CK, Kim SH. Ultrasound of the urinary bladder, revisited. *J Med Ultrasound*. 2007;15(2):77–90.
18. Pecoraro M, Takeuchi M, Vargas HA, et al. Overview of VI-RADS in bladder cancer. *Am J Roentgenol*. 2020;214(6):1259–68. <https://doi.org/10.2214/AJR.20.22763>.
19. Panebianco V, Narumi Y, Altun E, et al. Multiparametric magnetic resonance imaging for bladder cancer: development of VI-RADS (vesical imaging-reporting and data system). *Eur Urol*. 2018;74(3):294–306. <https://doi.org/10.1016/j.eururo.2018.04.029>.
20. Rafique M, Javed AA. Role of intravenous urography and transabdominal ultrasonography in the diagnosis of bladder carcinoma. *Int Braz J Urol*. 2004;30(3):185–91. <https://doi.org/10.1590/s1677-55382004000300002>.
21. Raman SP, Horton KM, Fishman EK. Transitional cell carcinoma of the upper urinary tract: optimizing image interpretation with 3D reconstructions. *Abdom Imaging*. 2012;37(6):1129–40. <https://doi.org/10.1007/s00261-011-9838-2>.
22. Galgano SJ, Porter KK, Burgan C, Rais-Bahrami S. The role of imaging in bladder cancer diagnosis and staging. *Diagnostics*. 2020;10(9):703. <https://doi.org/10.3390/diagnostics10090703>.
23. Chow LC, Kwan SW, Olcott EW, Sommer G. Split-bolus MDCT urography with synchronous nephrographic and excretory phase enhancement. *Am J Roentgenol*. 2007;189(2):314–22.
24. ●●Panebianco V, Pecoraro M, Del Giudice F, et al. VI-RADS for bladder cancer: current applications and future developments. *J Magn Reson Imaging*. 2022;55(1):23–36. <https://doi.org/10.1002/jmri.27361>. *An important reference which opens to current applications and future perspectives of the Vesical Imaging Reporting and Data System (VI-RADS).*
25. Ge X, Lan ZK, Chen J, Zhu SY. Effectiveness of contrast-enhanced ultrasound for detecting the staging and grading of bladder cancer: a systematic review and meta-analysis. *Med Ultrason*. 2021;23(1):29–35. <https://doi.org/10.11152/mu-2730>.
26. Gao RZ, Wen R, Wen DY, et al. Radiomics analysis based on ultrasound images to distinguish the tumor stage and pathological grade of bladder cancer. *J Ultrasound Med*. 2021;40(12):2685–2697. <https://doi.org/10.1002/jum.15659>.
27. Trinh TW, Glazer DI, Sadow CA, Sahni VA, Geller NL, Silverman SG. Bladder cancer diagnosis with CT urography: test characteristics and reasons for false-positive and false-negative results. *Abdom Radiol (NY)*. 2018;43(3):663–71. <https://doi.org/10.1007/s00261-017-1249-6>.
28. Garapati SS, Hadjiiski L, Cha KH, et al. Urinary bladder cancer staging in CT urography using machine learning. *Med Phys*. 2017;44(11):5814–23. <https://doi.org/10.1002/mp.12510> [25] July–Aug 2022;48(4):609–22. <https://doi.org/10.1590/S1677-5538.IBJU.2021.0560>. VI-RADS score system—a primer for urologists
29. Del Giudice F, Leonardo C, Simone G, et al. Preoperative detection of Vesical Imaging-Reporting and Data System (VI-RADS) score 5 reliably identifies extravesical extension of urothelial carcinoma of the urinary bladder and predicts significant delayed time to cystectomy: time to reconsider the need for primary deep transurethral resection of bladder tumour in cases of locally advanced disease? *BJU Int*. 2020;126(5):610–9. <https://doi.org/10.1111/bju.15188>.
30. El-Karamany TM, Al-Adl AM, Hosny MM, Eldeeb AH, El-Hamshary SA. Clinical utility of vesical imaging-reporting and data system (VI-RADS) in non-muscle invasive bladder cancer (NMIBC) patients candidate for en-bloc transurethral resection: a prospective study. *Urol Oncol*. 2022;40(10):4541–7. <https://doi.org/10.1016/j.urolonc.2022.03.008>.
31. Al Johi RS, Seifeldin GS, Moeen AM, et al. Diffusion weighted magnetic resonance imaging in bladder cancer, is it time to replace biopsy? *Cent Eur J Urol*. 2018;71(1):31–7. <https://doi.org/10.5173/cej.2017.1427>.
32. Necchi A, Bandini M, Calareso G, et al. Multiparametric magnetic resonance imaging as a noninvasive assessment of tumor response to neoadjuvant pembrolizumab in muscle-invasive bladder cancer: preliminary findings from the PURE-01 study.

- Eur Urol. 2020;77(5):636–43. <https://doi.org/10.1016/j.eururo.2019.12.016>.
33. Bricio TGM, Gouvea GL, Barros RV, et al. What is the impact of dynamic contrast-enhancement sequence in the Vesical Imaging, Reporting and Data System (VI-RADS)? A subgroup analysis. *Cancer Imaging*. 2022;22(1):20. <https://doi.org/10.1186/s40644-022-00459-1>. (Published 3 May 2022).
 34. Cai Q, Ling J, Kong L, et al. Multiparametric MRI evaluation of VI-RADS for bladder tumors located at the ureteral orifice. *Radiology*. 2022;304(3):593–9. <https://doi.org/10.1148/radiol.220028>.
 35. Séguier D, Puech P, Kool R, et al. Multiparametric magnetic resonance imaging for bladder cancer: a comprehensive systematic review of the Vesical Imaging-Reporting and Data System (VI-RADS) performance and potential clinical applications. *Ther Adv Urol*. 2021;13:17562872211039584. <https://doi.org/10.1177/17562872211039583>. Published 25 Aug 2021.
 36. Del Giudice F, Pecoraro M, Vargas HA, et al. Systematic review and meta-analysis of vesical imaging-reporting and data system (VI-RADS) inter-observer reliability: an added value for muscle invasive bladder cancer detection. *Cancers (Basel)*. 2020;12(10):2994. <https://doi.org/10.3390/cancers12102994>. (Published 15 Oct 2020).
 37. da Silva MC, Pecoraro M, Pesciotti ML, et al. The learning curve in bladder MRI using VI-RADS assessment score during an interactive dedicated training program. *Eur Radiol*. 2022;3:1. <https://doi.org/10.1007/s00330-022-08766-8>. (Published online ahead of print, 2 April 2022).

Publisher's Note, Springer Nature remains neutral with regard to jurisdictional claims in published maps and institutional affiliations.